

Assessment of the position and morphology of the condylar head of mandible after sagittal split ramus osteotomy: A postoperative comparative study from 1 to 6 months

Ryutaro Imamura^a

^{a)} Graduate Student, Department of Orthodontics, Nihon University School of Dentistry at Matsudo, Chiba, Japan

Abstract

Sagittal split ramus osteotomy (SSRO) is widely used for skeletal mandibular prognathism, but various changes are seen after SSRO. Changes in the position of the mandible immediately after surgery can lead to unstable occlusion and prolonged orthodontic treatment. The aims of this study were to examine the changes in the positions of the proximal fragment and the condylar head of the mandible and to investigate the morphological changes in the condylar head of the mandible using CT images acquired before SSRO (BO) and 1 month (AO1) and 6 months (AO6) after SSRO.

1. Significant changes in the axial condylar angle were found at BO-AO1 and at BO-AO6.

However, significant changes in measurements on the coronal plane were not found at BO, AO1, or AO6. Significant changes in the distance between the mandibular fossa and the condylar head of the mandible on the axial plane were also not found at BO, AO1, or

AO6.

2. There were significant differences in the proximal fragment along the X-axis and Z-axis from BO to AO1. There was no significant difference in the proximal fragment from AO1 to AO6.
3. The height (SH and CH) of the condyle was significantly decreased from AO1 to AO6.
4. Changes of the proximal fragment along the X-axis were correlated with the width of the condyle, and changes along the Y-axis were inversely correlated with height, sagittal width, and axial width of the condyle. Changes of the proximal fragment along the Z-axis were inversely correlated with the axial width of the condyle.
5. Reductional bony change was found in areas B, C, E, and F, while additional bony change was found in areas B and G.

In conclusion, external and superior displacement of the proximal fragment and positional changes of the condylar head of the mandible due to external, superior, and internal rotation often occurred immediately after SSRO. It was suggested that bone remodeling was found from the external surface of the condylar head of the mandible to its antero-superior aspect.

Introduction

Sagittal split ramus osteotomy (SSRO) is widely used to treat skeletal mandibular prognathism. There are many reports about the factors related to various changes after SSRO¹⁻⁴⁾. Factors that produce changes immediately after SSRO presumably differ from those that produce changes over the long term. In particular, positional changes of the mandible immediately after surgery can cause unstable occlusion and necessitate prolonged postoperative orthodontic treatment.

Various studies have examined the changes in the mandibular bone fragment after SSRO^{5,6)}. They have reported that the positional changes of the mandible were primarily due to the traction exerted by the masticatory muscles, such as the lateral pterygoid, mesial pterygoid, and masseter. Okuda et al.⁶⁾ reported that the occlusal force and the force exerted by jaw depressors were concentrated on the site of osteosynthesis, thus causing reversion after SSRO. Okuda et al. also reported that the position of the bone fragment could change within 6 months after surgery. Mizuno et al.⁷⁾ examined changes in the mandible of patients who underwent SSRO to correct skeletal mandibular prognathism and found that the extent of setback due to surgery and the extent of relapse after surgery were closely correlated. Mizuno et al. ascribed this correlation to various factors, such as postoperative occlusion, the path of the muscles, the morphology of the condylar head of the mandible and mandibular fossa, the position of the mandible, and jaw movement.

Previous studies have examined the positional changes of the condylar head of the mandible after SSRO in 2 dimensions (2D). Kawamura et al.⁸⁾ used CT images to measure the distance between the condylar head of the mandible and the mandibular fossa on frontal and sagittal sections, and they described the positional changes of the condylar head of the mandible. Therefore, some studies¹⁻⁹⁾ have assessed the bone fragment before and after SSRO and the displacement of the condylar head of the mandible in 2D. With 2D measurement, it is difficult to describe changes in position and morphology of the condylar head of the mandible in detail, and 3-dimensional (3D) analysis is considered necessary. However, there have been few studies evaluating displacement of the bone fragment and the position and morphology of the condylar head of the mandible in three dimensions^{24, 25, 28)}.

The aims of this study were to examine the changes in the positions of the proximal fragment and the condylar head of the mandible and to investigate the morphological changes in the condylar head of the mandible using CT images acquired before SSRO (BO), 1 month (AO1) , 6 months (AO6) after SSRO.

Materials and Methods

1. Subjects

The subjects were 23 patients (9 males, 14 females; mean \pm SD age: 27.3 ± 7.4 years) who were diagnosed with skeletal mandibular prognathism by orthodontists of the Nihon University Hospital at Matsudo. These patients underwent orthognathic surgery in the form of SSRO by the Department of Maxillofacial Reconstruction, Nihon University Hospital at Matsudo. All procedures were performed by the same surgeon. The mean setback distance was 9.7 ± 3.2 mm.

Exclusion criteria: patients with occlusal instability after surgery; patients with a 1 mm or greater gap of centric occlusion and centric relation; patients with marked facial asymmetry; and patients with masticatory muscle pain, temporomandibular joint pain, joint sounds, and impaired jaw movement.

This study was approved by the Ethics Committee of Nihon University's School of Dentistry at Matsudo (approval no.: EC 16-14-041-1).

2. Reproducibility of measurement

Reproducibility of measurement points and the imaging method was examined by a preliminary experiment using a dry skull following the method of Endo et al.⁹⁾ The error between the measured value on the 3D CT image and the actual measured value was analyzed. In actual measurement, using the software used in the preliminary experiment, all measurements in this study were made by the same individual. All measurements were made

in duplicate, and measurement reproducibility was examined. Measurement followed the double determination method of Dahlberg et al.⁹⁾.

To assess the significance of the error involved in the 3D-CT measurement methods, the authors re-assessed a series of 20 subjects two months after the initial measurements were taken. In the preliminary experiment, the coefficients of variation were 0.39-1.89%. In measuring patient data, the coefficients of variation of the coordinate value and the distance measurement were 0.51-2.13% and 0.54-2.21%, respectively. The values showed good reproducibility.

3. Maxillofacial 3D-CT images

CT images were used to measure the distance between the condylar head of the mandible and the mandibular fossa in the coronal and axial planes. CT images were also used to create maxillofacial 3D-CT images, and the extent of changes in the proximal fragment and the extent of morphological changes in the condylar head of the mandible were measured. In addition, the distribution of remodeling of the condylar head of the mandible was determined using maxillofacial 3D-CT images.

3-1) Reconstructing 3D-CT image

CT images acquired before SSRO (BO), 1 month after SSRO (AO1), and 6 months after surgery (AO6) were used. The images were obtained using an Aquilion 64 CT scanner (Toshiba Medical Systems, Tokyo, Japan) at this hospital. The imaging parameters were as follows: tube voltage, 120 kV; tube current 100 mA; field of view, 240 mm × 240 mm; and slice thickness, 1 mm. The scanning range was from the forehead to the chin. The position of

the patient's head was set using a positioning laser. The longitudinal axis of the beam was the front of the face, and the horizontal axis of the beam was a plane connecting the tragus and left orbit. Occlusion was imaged at the maximal intercusp position, with the lips gently closed. After image acquisition, the acquired CT data were imported and converted to the DICOM format and then to the standard triangulated language (STL) format using DICOM viewer software (OsiriX, Newton Graphics, Hokkaido, Japan). Data were thresholded using 3D volume rendering software (Artec Studio 9, Artec 3D, Luxembourg City, Luxembourg). The skull and mandible were rendered, and 3D-CT images were reconstructed.

3-2) Definition of the spatial coordinate system for the 3D CT image

Standard coordinates were set for 3D image data in the STL format using 3D image analysis software (Body-Rugle, Medic Engineering, Kyoto, Japan). The coordinates were based on the upper margin of the porions (Po) of the left and right external auditory canals and the right infraorbital margin orbitale (Or) on maxillofacial skeletal 3D-CT images. The plane defined by the Po on both the left and right sides and the Or served as the Frankfurt horizontal (FH) plane (defined here as the axial plane). The plane passing through the Po on both the left and right sides and perpendicular to the axial plane served as the coronal plane. The plane passing through the center of the Po on the left and right sides and perpendicular to the axial plane served as the sagittal plane. A straight line passing through the Po on the left and right sides served as the X-axis. A straight line passing through the center of the Po on

the left and right sides and perpendicular to the FH plane served as the Y-axis. A straight line passing through the origin and perpendicular to the X-axis served as the Z-axis (Fig. 1). The left side of the X axis is (+), the upside of the Y axis is (+), and the anterior side of the Z axis is (+).

Liner and angular measurements using 3D images were analyzed, and calculated automatically on the computer.

4. Measurement

4-1) Measurement of the distance between the mandibular fossa and the condylar head of the mandible

The distance from the mandibular fossa to the condylar head of the mandible was measured on the coronal and axial planes at BO, AO1, and AO6. The landmarks for the condylar head of the mandible and the mandibular fossa and the measurement points on the coronal plane were set. A straight line connecting the most lateral point (LP) and the most medial point (MP) of the condylar head of the mandible was divided into 6 equal sections. The more LP was defined as the coronal lateral point (CL), the central point was defined as the coronal central point (CC), and the more MP was defined as the coronal medial point (CM). The point representing the shortest distance from CL to the mandibular fossa was designated the lateral space (LS), the point representing the shortest distance from CC to the mandibular fossa was designated the central space (CS), and the point representing the

shortest distance from CM to the mandibular fossa was designated the medial space (MS). The distances LS-CL, CS-CC, and MS-CM were measured (Fig. 2)⁸⁾. The angle formed by a straight line passing through LP-MP and the FH plane represented the coronal condylar angle (Fig. 3)⁸⁾.

LP and MP of the condylar head of the mandible on the axial plane were identified. The point representing the shortest distance from the LP to the mandibular fossa was designated the axial lateral space (ALS), and the point representing the shortest distance from the MP to the mandibular fossa was designated the axial medial space (AMS). The distances LP-ALS and MP-AMS were measured (Fig. 4)⁸⁾. In addition, the length of a straight line connecting the LPs of the left and right condylar heads of the mandibles was measured as the distance MSR-Condyle, and the angle formed by the intersection of the straight line LP-MP on the left and right condylar heads of the mandibles was measured as the axial condylar angle (Fig. 5)⁸⁾.

4-2) Measurement of changes in the proximal bone fragment and condylar head of the mandible

Three-dimensional CT images at BO, AO1, and AO6 were overlaid, and the extent of changes in the proximal fragment and condylar head of the mandible was measured. In order to measure the extent of changes in the proximal fragment, 3D-CT images of the chin were overlaid in 3D image analysis software (Body-Rugle, Medic Engineering) using the least

squares method. The software used an algorithm based on mutual information in a region to calculate the optimal position. The most lateral point of the condylar head of the mandible (Lp), sigmoid notch (Sn), coronoid process (Cp), and antegonial notch (An) served as the landmarks for the proximal fragment, and the extent of displacement was determined on the coordinate axes (Figs. 6,7).

4-3) Changes condylar head of the mandible from AO1 to AO6

In order to measure the extent of changes in the condylar head of the mandible, the images were similarly overlaid on the basis of the ramus of the mandible. The extent of changes in the condylar head of the mandible was measured in 3 sections: the sagittal plane, axial plane, and coronal plane. The most anterior point of the condylar head of the mandible (AP), the most posterior point of the condylar head of the mandible (PP), and the highest point of the condylar head of the mandible (CoT) were measured on the sagittal plane, and the length of AP-PP (sagittal width (SW)) and the distance from CoT to AP-PP (sagittal height (SH)) were measured. The MP and LP were measured on the axial plane, and the length of MP-LP (axial width (AW)) and the distance through the center perpendicular to MP-LP (axial depth (AD)) were measured. MP, LP, and CoT were measured on the coronal plane, and the length of MP-LP (coronal width (CW)) and the distance from CoT to MP-LP (coronal height (CH)) were measured (Fig. 8).

4-4) Correction between displacement of proximal bone fragment from BO to AO1 and change of the condylar head from AO1 toAO6

The extent of changes in the proximal fragment and the extent of morphological changes in the condylar head of the mandible were measured. The measurement points of the proximal bone fragment were Lp, Sn, Cp, and An. The measurement points of the condylar head were SW, SH, AW, AD, CW, CH. Whether the movement of the proximal bone fragment from BO to AO1 was related to the change of which part of the condylar head from AO1 toAO6 were evaluated by Pearson 's correlation coefficients.

4-5) Remodeling of the condylar head of the mandible

Remodeling at BO and AO6 was compared, and sites where remodeling had occurred were determined. LP and MP of the condylar head of the mandible from the axial plane served as the long axis, and a straight line perpendicular to that axis was divided into 3 equal sections. Sections were divided into 9 areas: Anteromedial (A), Antero-middle (B), Anterolateral (C), Medial (D), Middle (E), Lateral (F), Posteromedial (G), Posteromiddle (H), and Posterolateral (I) (Fig. 9). The changes of the condylar head were evaluated by the least squares method of the 3D-superimposition software (Body-Rugle, Medic Engineering) using the mandibular ramus area. The changes of the condylar head were demonstrated using a color scale. Nine areas of 46 condyles of 23 subjects were classified into unchanged(less than $\pm 0.5\text{mm}$), additional bony change ($+0.5\text{mm}$ or more) and reductional bony change

(-0.5mm or less) . The differences in the distance between AO1 and AO6 in the 3D mesh data of condylar head were indicated by color scale. The range of less than ± 0.5 mm was displayed in gray and represents unchanged. The additional bony change of 0.5 mm or more was indicated in red. The reductional bony change by -0.5 mm or less was indicated in blue. Chi-square test was performed to compare the ratio of reductional bony change and the ratio of additional bony change in each area.

5. Statistical analysis

The position of the temporomandibular joint, distances between the measurement points, angular measurements, the positional changes of the proximal fragment, and morphological changes of the condylar head of the mandible were compared using the paired *t*-test and repeated measures ANOVA. The changes in the proximal fragment and condylar head of the mandible were assessed using Pearson's correlation coefficients. The distribution of remodeling of the condylar head of the mandible was determined on the basis of bone resorption in each areas and the ratio of areas with bone apposition with respect to areas without changes. Chi-square test was performed to compare the ratio of reductional bony change and the ratio of additional bony change in each area.

Results

1. Distance between the mandibular fossa and the condylar head of the mandible

There was no significant difference in line and angular measurements on the coronal plane (Table 1). There were no significant changes between the variables of the mandibular fossa and those of the condylar head of the mandible on the axial plane (Table 2). However, there were significant decreases ($p < 0.05$) in the axial condylar angle between BO and AO1, and between BO and AO6 on the axial plane (Table 2).

2. Displacement of the proximal bone fragment

On the displacement between BO and AO1, there was significant decrease in Lp on right and left sides along the X-axis ($p < 0.05$), on the contrary, there was no significant difference in other measurements (Table 3). On the displacement between AO1 and AO6, there was no significant difference in each measurement (Table 4). Comparing two type of fixation, there was no significant difference between biodegradable plate and titanium plate (Table 4).

3. Changes of the condylar head of the mandible at AO1 and AO6

Significant decreases in SH and CH were found from AO1 to AO6 ($p < 0.05$). Therefore, the height of the condyle was significantly decreased from AO1 to AO6. There were no significant differences between AO1 and AO6 in other measurements (Table 5).

4. Correlation coefficient between the displacement amount of the proximal bone fragment and changes of the condylar head of the mandible

Changes of Cp along the X-axis were correlated with CW. Changes of Cp along the Y-axis were inversely correlated with AD, CW and CH. Changes of Cp along the Z-axis were inversely correlated with AW. (Table 6)

Changes of Lp of the proximal fragment along the X-axis were inversely correlated with SW, AD and CW.

Changes of Sn of the proximal fragment along the Y-axis were inversely correlated with SH and AD. Changes of An of the proximal fragment along the X-axis were inversely correlated with CH. Changes of An along the Y-axis were closely inversely correlated with SH, AD, CW, and CH.

5. Remodeling of the condylar head of the mandible

Unchanged was the most frequent in all areas. Chi-square test was performed to compare the ratio of reductional bony change and the ratio of additional bony change in each area. Reductional bony change were found in areas B, C, E, and F, while signs of additional bony change were found in areas D and G (Table 7).

Discussion

Studies have shown that distinct double lines depicting the condylar head of the mandible on a cephalogram after SSRO indicate remodeling of the condylar head of the mandible and mandibular fossa¹⁰⁻¹⁴). However, these studies involved 2D analysis and X-ray analysis; therefore, correctly ascertaining displacement in 3 dimensions or the manner of remodeling was difficult. Over the past few years, the use of high-speed spiral CT has become widespread, and it provides 3D data in a short time. This has facilitated 3D reconstruction of the temporomandibular joint¹⁵⁻¹⁷).

In the present study, the proximal fragment was displaced laterally. This caused the condylar head of the mandible to be located more externally, and it caused the medial aspect of the condylar head to rotate more internally (Fig. 7). These findings are presumably a result of positioning of the proximal fragment during surgery and changes in the path of the lateral pterygoid and masseter. The lateral pterygoid is attached to the condylar head of the mandible, and the masseter is attached to the masseteric tuberosity at the angle of the mandible. External displacement of the proximal fragment involves internal traction of the lateral pterygoid and upward traction of the masseter^{4-6,18-19}).

The present results indicated that the extent to which the medial aspect of the condylar head of the mandible rotates internally in the mandibular fossa after surgery is a predictor of remodeling²⁰⁻²²).

A previous study reported that remodeling of the condylar head was influenced by factors

such as age in the long-term cases over a year or more after surgery. However, remodeling was found in a short period of time, i.e., from AO1 to AO6, which was presumably the result of external and internal rotation of the condylar head of the mandible.

Studies that analyzed conventional lateral cephalograms found bone resorption resembling remodeling on the anterosuperior and lateral aspects of the condylar head of the mandible after orthognathic surgery²⁴⁻²⁶⁾. The present study analyzed 3D-CT and obtained similar results for the same regions. Remodeling of the condylar head of the mandible can be attributed to mechanical stress²⁷⁾. This may be because the position of the condylar head of the mandible changes after SSRO and is caused by mechanical adaptation after surgery.

Reductional bony change was often found from the external surface to the anterior and anterosuperior aspects of the condylar head of the mandible. In addition, the current results suggest that resorption occurred on the superior and lateral aspects of the condylar head of the mandible when the proximal fragment was substantially displaced superiorly and externally. The condylar head was covered by the articular capsule and tight ligaments, such as the lateral ligament. External movement of the condylar head of the mandible presumably resulted in additional bony change in the sustained load on the lateral aspect of the condylar head of the mandible²⁸⁻³⁰⁾.

Bone apposition, albeit slight, was found on the posterior aspect of the condylar head of the mandible and particularly on the medial aspect. The findings of bone apposition was

found in a position relative to where bone resorption occurred. Changes in the position of the condylar head of the mandible occurred because of the expansion of the temporomandibular joint space²⁹⁾.

Displacement of the proximal fragment and positional and morphological changes of the condylar head of the mandible were found, but none of the patients had joint symptoms or dysfunction after surgery. This is presumably caused by positional changes of the condylar head of the mandible after SSRO were within the range of adaptation or because remodeling occurred to facilitate adaptation. Nonetheless, the extent of adaptation and risk factors affecting adaptation warrant further study in the future.

Conclusion

External and superior displacement of the proximal fragment and changes in the position of the condylar head of the mandible with external, superior, and internal rotation occurred often immediately after SSRO. It was suggested that bone remodeling was found from the external surface of the condylar head of the mandible to its anterosuperior aspect.

References

- 1) Sugiyama N, Morita S, Mise Y, Saito C, Takagi R, Saito I: Postoperative changes in skeletal mandibular progenitor cases with upper and lower jaw movement surgery. *The Journal of Kouhokushinetsu Orthodontic Society*, 20: 25-33, 2012.
- 2) Ishiyama C, Sueishi K, Yamaguchi H, Suzuki T, Arakawa Y: Long-term Stability of Surgical Treatment Cases of Skeletal Mandibular Prognathism. *Jpn. J. Jaw*, 13: 111-117, 2002.
- 3) Feinerman DM, Piecudh JF: Long-term effect of orthodontic surgery on the temporomandibular joint: comparison of rigid and nonrigid fixation methods. *Surg*, 24: 268-272, 1995.
- 4) Takashi K, Suzuki T, Higuchi K, Mita K, Toneki S, Suzuki K, Tsuruki T, Ichinokawa Y, Nomura M, Yamaguchi H: Long-term Stability of Surgical Treatment Cases of Skeletal Mandibular Prognathism. *The Japanese Journal of Jaw Deformities*, 102: 583-596, 2002.
- 5) Ana LL, Walter LM, Antonio CO, Margareth MG, Lincoln I N: Long-term skeletal and profile stability after surgical-orthodontic treatment of Class II and Class III malocclusion. *Journal of Cranio-Maxillo-Facial Surgery*, 41: 296-302, 2013
- 6) Okuda K, Nakazima M, Kakudou K: Biomechanical analysis of the effect of occlusal force on osteosynthesis following sagittal split ramus osteotomy. *Journal of Osaka*

- Odontological Society, 72: 9-17, 2009.
- 7) Kai K, Takeyama M, Saito I, Morita S, Hanada K: Long-term dental arch changes after sagittal splitting ramus osteotomies in skeletal Class III malocclusions. Niigata Dental Journal, 31: 167-172, 2001.
 - 8) Ikeda K, Kawamura A: Assessment of Optimal Condylar Position in the Coronal and Axial Planes with Limited Cone-Beam Computed Tomography. American college of prosthodontists, 20: 432-438, 2011
 - 9) Endo M, Terajima M, Goto K, Tokumori K, Takahashi I: Three-dimensional analysis of the temporomandibular joint and fossa-condyle relationship. Orthodontics, 12: 210-221, 2011.
 - 10) Dahlberg G. Statistical methods for medical and biological students. London: George Allen and Unwin Ltd. 1940: 122-132.
 - 11) Chiung SH, Glenda H, Eric JW, Chen YR: Mandibular remodeling after bilateral sagittal split osteotomy for prognathism of the mandible. J Oral Maxillofac Surg, 64: 167-172, 2006.
 - 12) Katsumata A, Nojiri M, Fujishita M, Ariji Y, Ariji E, Langlais RP: Condylar head remodeling following mandibular setback osteotomy for prognathism: a comparative study of different imaging modalities. Oral Surg Oral Med Oral Pathol Oral Radiol Endod, 101: 505-514, 2006.

- 13) Petersson A, Willimar HK: Radiographic changes of the temporomandibular joint after oblique oblique sliding osteotomy of the mandibular rami. *Surg*, 18: 27-31, 1989.
- 14) Fred LH, Joseph E, Pirkka V: Condylar displacement and temporomandibular joint dysfunction following bilateral sagittal split osteotomy and rigid fixation. *J Oral Maxillofac Surg*, 47: 223-227, 1989.
- 15) Kenneth SR, Herbosa EG, Nickels B: Correction of condylar displacement following intraoral vertical ramus osteotomy. *J Oral Maxillofac Surg*, 49 :366-372, 1991.
- 16) Mohammad BM, Dumas AL, Chavoor AG, Neff PA, Homayoun N: Temporomandibular joint: Computed tomographic three-dimensional reconstruction. *Am J Ortod*, 88: 342-352, 1985.
- 17) Usami H, Mori T, Kawaguchi T, Oyama N, Katoh E, Takahama Y, Naitoh M: A new method for measuring three-dimensionally the joint space using a TMJ digital reconstruction technique. *J.Jpn.Soc.Stomatognath*, 6: 11-18, 1999.
- 18) Timmis DP, Aragon SB, Van Sickels JE: Masticatory dysfunction with rigid and nonrigid osteosynthesis of sagittal split osteotomies. *Oral Surg Oral Med Oral Pathol*, 62: 119-123, 1986.
- 19) Paulus GW, Steinhauser EW: A comparative study of wire osteosynthesis versus bone screws in the treatment of mandibular prognathism. *Oral Surg Oral Med Oral*

- Pathol, 54: 2-6, 1982.
- 20) Papachristou DJ, Papachroni KK, Papavassiliou GA, Pirttiniemi P, Gorgoulis VG, Piperi C, Efthimia KB: Functional alterations in mechanical loading of condylar cartilage induces changes in the bony subcondylar region. *Arch Oral Biol*, 54: 1035-1045, 2009.
- 21) Eckerdal O, Sund G, Astrand P: Skeletal remodelling in the temporomandibular joint after oblique sliding osteotomy of the mandibular rami. *Int J Oral Maxillofac Surg*, 15: 233-239, 1986.
- 22) Ruf S, Pancherz H: Temporomandibular joint remodeling in adolescents and young adults during Herbst treatment: A prospective longitudinal magnetic resonance imaging and cephalometric radiographic investigation. *Am J Orthod Dentofacial Orthop*, 115: 607-618, 1989.
- 23) Moore KE, Gooris PJ, Stoelinga PJ: The contributing role of condylar resorption to skeletal relapse following mandibular advancement surgery: report of five cases. *J Oral Maxillofac Surg*, 49:448-60, 1991.
- 24) Christian SR, Antonio R, Arthur M, Katherine K, Joni LR, Lucia C: Congenital and acquired mandibular asymmetry: Mapping growth and remodeling in 3 dimensions. *Am J Orthod Dentofacial Orthop*, 150: 238-251, 2016.
- 25) Ooyama T: Three-Dimensional Reconstruction of the Temporomandibular Joint

- Using CT and Analysis of Mandibular Movements. The Aichi-Gakuin Journal of Dental Science, 34: 193-201, 1996.
- 26) Kerstens HC, Tuinzing DB, Golding RP, van der Kwast WA: Condylar atrophy and osteoarthritis after bimaxillary surgery. Oral Surg Oral Med Oral Pathol, 69: 274-280, 1990.
- 27) Mongini F: Condylar remodeling after occlusal therapy. J Prosthet Dent, 43: 568-577, 1980.
- 28) Kinzinger G, Kober C, Diedrich P: Topography and morphology of the mandibular condyle during fixed functional orthopedic treatment-a magnetic resonance imaging study. J Orofac Orthop, 68: 124-147, 2007.
- 29) Takahashi A, Matsumoto N, Yotsui Y: Stomatognathic function and image evaluation for skeletal mandibular protraction case with remarkable remodeling on the condyle. J. Jpn Soc. TMJ, 20: 239-244, 2008.
- 30) Sakai Takeo, Kawata Mituhiro: Prometheus. Igaku-shoin, 1: 32-35, 2009.

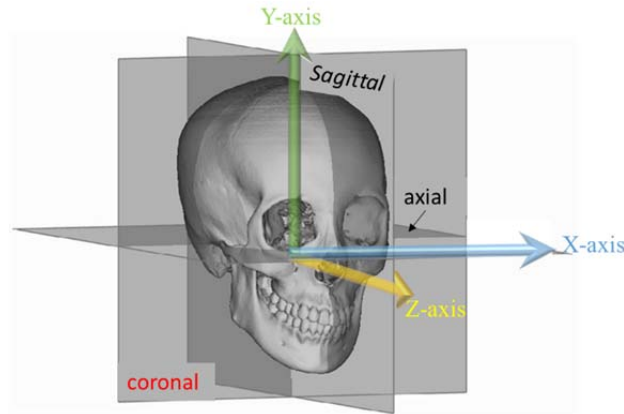


Fig.1 Definition of the spatial coordinate system for the 3D CT image.

The Frankfort horizontal (axial) plane (X-axis) was defined by the right and left porions and the center of the right and left orbitales. The coronal plane (Y-axis) was perpendicular to the axial plane, passing through the right and left porions. The sagittal plane (Z-axis) was perpendicular to the axial and coronal planes, passing through the center of the right and left orbitales. The left side of the X axis is (+), the upside of the Y axis is (+), and the anterior side of the Z axis is (+).

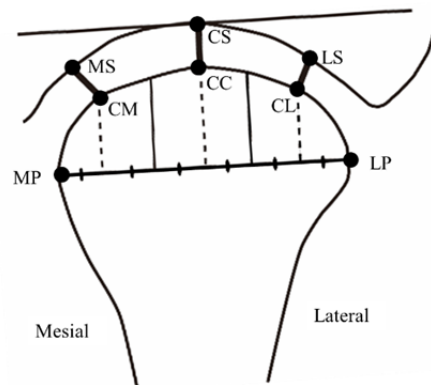


Fig.2 Landmarks and linear measurements of the space between the condyle and the glenoid fossa.

Line connecting the most lateral point (LP) and the most medial point (MP) was equally divided into 6 and lateral point is referred as the coronal lateral point (CL), midpoint as the coronal central point (CC), mesial point as the coronal medial point (CM) on a coronal plane. On a glenoid fossa, the lateral space (LS), the central space (CS), the medial space (MS) indicates points of shortest distance from CL, CC, and CM, respectively. Distances of LS-CL, CS-CC, and MS-CM were measured.

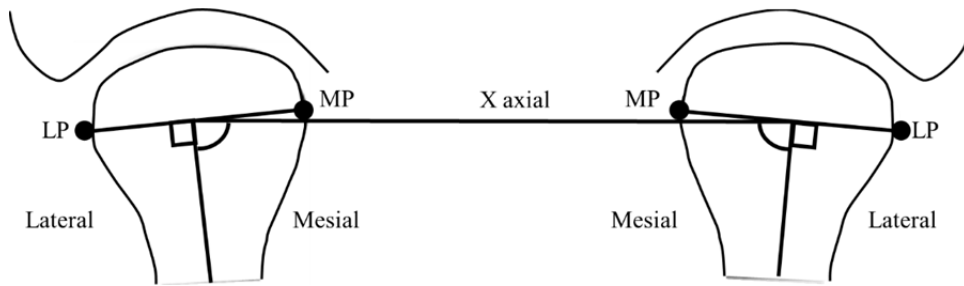


Fig.3 Landmarks and angular measurements of the condylar heads of mandible on a coronal plane.

The angle between the line which go through the most lateral point (LP) and the most medial point (MP) and Frankfurt plane was measured as coronal condylar angle.

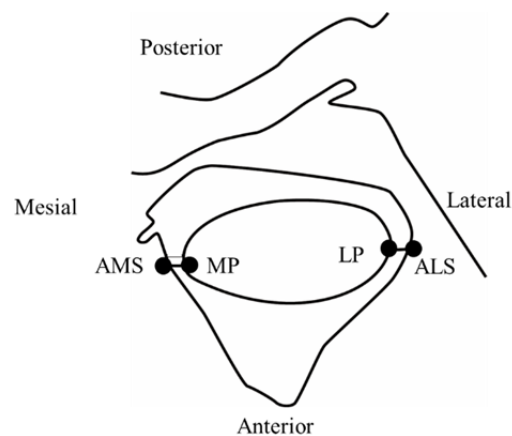


Fig.4 Landmarks and linear measurements of the space between the condyle and the glenoid fossa on a axial plane.

Lateral point (LP) and mesial point (MP) of mandibular condyle was defined on a axial plane. The axial lateral space (ALS) and the axial medial space (AMS) were corresponded as the shortest distance from the most lateral point (LP) and the most medial point (MP) respectively. Distances of LP-ALS, MP-AMS were measured.

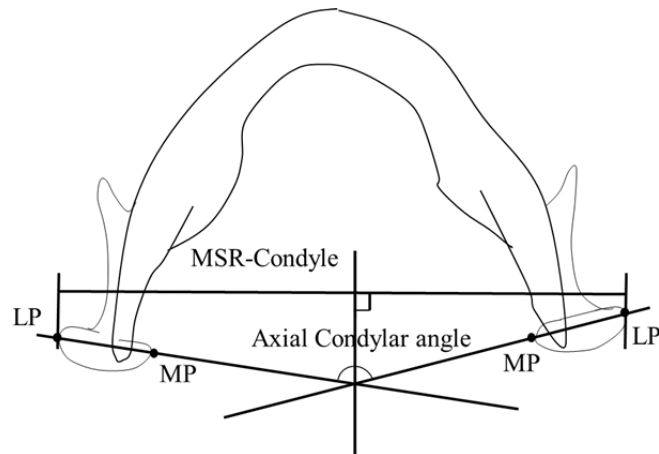


Fig.5 Landmarks and angular measurement of the condylar head of mandible on a axial plane.

LP : The most lateral point, MP : The most mesial point

Line connecting both points of the most lateral point (LP) on mandibular condyle was measured as distance of the most spacious range (MSR)-Condyle. The angle crossing LP-MP was measured as Axial Condylar angle.

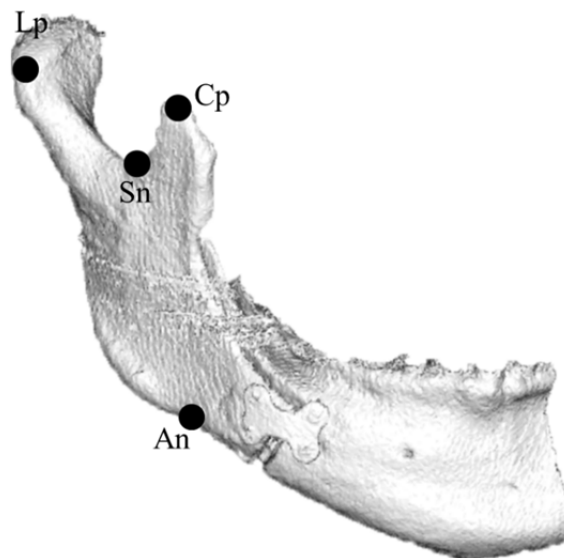


Fig.6 The landmarks of proximal fragment

Lp : Lateral point of condyle on a sagittal plane

Sn : Sigmoid notch

Cp : Coronoid process

An : Antegonial notch

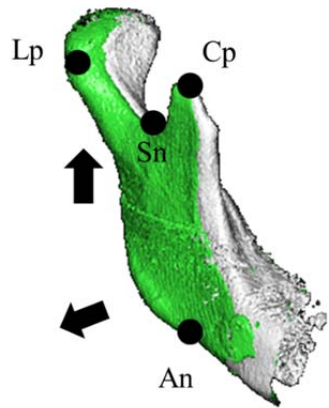


Fig.7 Displacement of the proximal bone fragment

Lp : Lateral point of condyle on a sagittal plane, Sn : Sigmoid notch

Cp : Coronoid process, An : Antegonial notch

Measure the extent of changes in the proximal fragment, 3D-CT images of the chin were overlaid in 3D image analysis software (Body-Rugle, Medic Engineering) using the least squares method. The proximal bone fragment of BO displayed in gray, and that of AO1 was displayed in green.

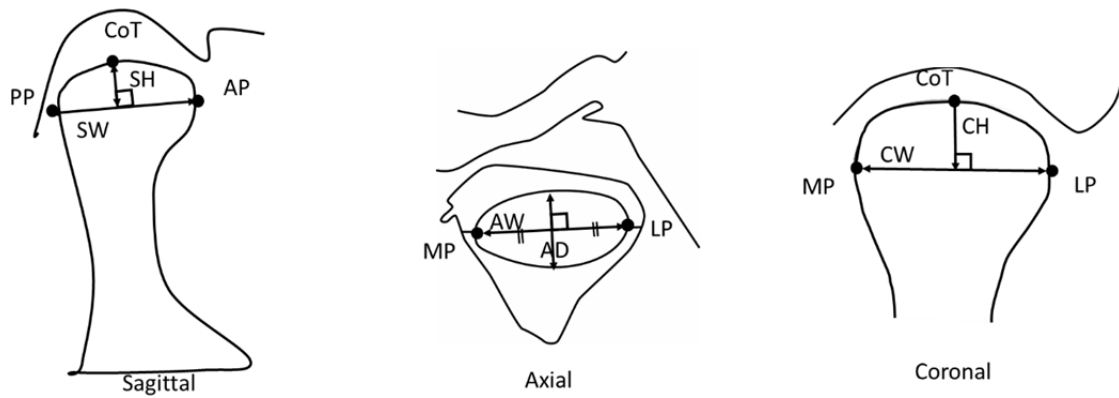


Fig.8 Landmarks and linear measurements of the condyle from three directions

Sagittal direction : Points are referred as the most anterior point of the head of the mandible (AP), the most posterior point of the head of the mandible (PP), and the highest point of the head of the mandible (CoT). Distance of AP-PP (SW) and line going through Cot and AP-PP (SH) were measured. Axial direction : Points are referred as the most medial point of the head of the mandible (MP) and the most lateral point of the head of the mandible (LP) . Distance of MP-LP (AW) and line crossing middle point of MP-LP (AD) were measured. Coronal direction : Points are referred as the most lateral point of the head of the mandible (LP), and the highest point of the head of the mandible (CoT) . Distance of MP-LP (CW) and line going through Cot and MP-LP (CH) were measured.

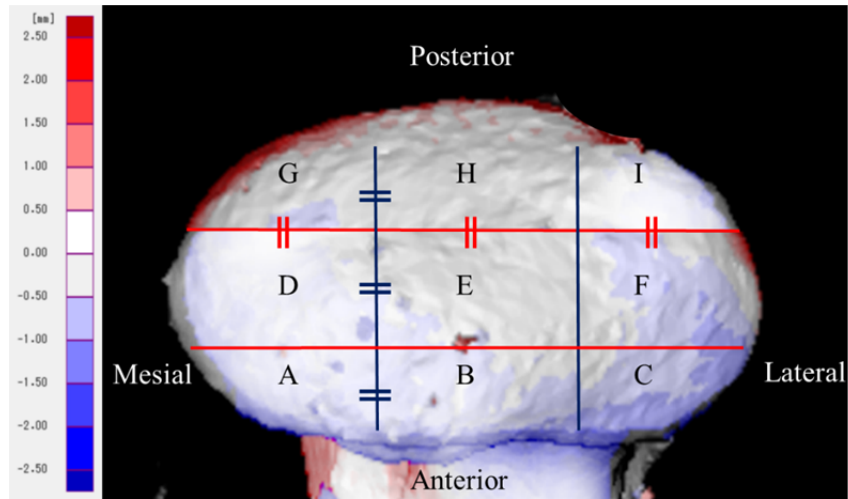


Fig.9 Remodeling of the condylar head of mandible from AO1to AO6

A : Anteromedial, B : Antero-middle, C : Anterolateral

D : Medial E:Middle, F : Lateral G : Posteromedial, H : Postero-middle, I : Posterolateral

The changes of the condylar head was evaluated by the least squares method that belong to 3D-superimpose software (Body-Rugle, medic Engineering) using mandibular ramus area. The changes of the condylar head were demonstrated by color scale.

The differences in the distance between AO1 and AO6 in the 3D mesh data of condylar head were indicated by color scale. The range of less than ± 0.5 mm is displayed in gray and represents unchanged. Additional bony change of 0.5 mm or more is indicated in red. Reductional bony change of -0.5 mm or less was indicated in blue.

Table 1 Condylar head measurements on a coronal plane

	BO		AO1		AO6	
	Mean	S.D.	Mean	S.D.	Mean	S.D.
Linear measurement (mm)						
LS-CL (right)	2.5	0.6	2.3	0.4	2.4	0.9
LS-CL (left)	2.6	0.8	1.8	0.6	1.9	0.8
CS-CC (right)	2.2	0.8	1.9	0.3	2.0	0.9
CS-CC (left)	2.0	0.5	1.5	0.4	1.7	0.7
MS-CM (right)	1.7	0.6	2.3	0.5	2.2	0.4
MS-CM (left)	1.3	0.3	1.7	0.6	1.7	0.6
Angular measurement (degree)						
Coronal Condylar angle (right)	81.2	4.2	80.8	0.4	80.3	4.6
Coronal Condylar angle (right)	83.1	3.8	83.0	0.5	82.7	3.9

BO : Before SSRO, AO1 : 1 month after SSRO, AO6 : 6 months after SSRO

CL : Coronal lateral point, CC : Coronal central point, CM : Coronal medial point

LS : Lateral space, CS : Central space, MS : Medial space

Coronal condylar angle : A straight line passing through LP-MP and the FH plane represented

Table 2 Condylar head measurements on a axial plane

	BO		AO1		AO6	
	Mean	S.D.	Mean	S.D.	Mean	S.D.
Linear measurement (mm)						
LP-AMS (right)	2.4	0.9	2.1	0.4	2.2	0.9
LP-AMS (left)	2.6	0.8	1.8	0.6	1.9	0.8
MP-ALS (right)	1.8	0.4	1.9	0.3	1.9	0.9
MP-ALS (left)	2.3	0.5	2.7	0.4	2.6	0.7
MSR-Condyle (right)	51.2	2.0	51.3	0.5	51.6	0.4
MSR-Condyle (left)	53.2	2.5	53.2	0.6	53.2	0.6
Angular measurement (degree)						
Axial Condylar angle (right)	77.1	5.6	72.1	0.4	73.5	4.6
Axial Condylar angle (left)	78.3	7.2	72.5	0.5	74.2	3.9

* $p < 0.05$ repeated measure ANOVA

BO : Before SSRO, AO1 : 1 month after SSRO, AO6 : 6 months after SSRO

LP : Lateral point, MP : Medial point, ALS : Axial lateral space, AMS : Axial medial space

MSR-Condyle : Length of a straight line connecting the LP of the left and right condylar head of mandibles

Axial condylar angle : The straight line LP-MP on the left and right condylar head of mandibles

Table 3 Displacement of proximal bone fragment from BO to AO1

		X		*	Y		Z	
		Mean	S.D.		Mean	S.D.	Mean	S.D.
Right	Cp	-1.5	1.1		0.9	0.4	1.0	0.4
	Lp	-2.3	0.9	*	1.8	0.6	0.9	0.6
	Sn	-1.5	0.5		0.9	0.3	0.8	0.4
	An	-1.9	0.6		1.1	0.4	0.9	0.4
Left	Cp	1.7	1.2		0.8	0.5	0.9	0.5
	Lp	2.6	1.0	*	1.9	0.6	1.2	0.7
	Sn	1.5	0.4		0.8	0.4	1.0	0.6
	An	2.0	0.7		1.1	0.5	0.9	0.4

* $p < 0.05$ paired *t*-test

(mm)

BO : Before SSRO, AO1: 1 month after SSRO

Lp : Most lateral point of the condylar head of mandible, Sn : Sigmoid notch

Cp : Coronoid process, An : Antegonial notch

Table 4 Displacement of proximal bone fragment from AO1 to AO6

		Total (n = 23)						Biodegradable Plates(n = 15)						Titanium Plates(n = 8)					
		X		Y		Z		X		Y		Z		X		Y		Z	
		Mean	S.D.	Mean	S.D.	Mean	S.D.	Mean	S.D.	Mean	S.D.	Mean	S.D.	Mean	S.D.	Mean	S.D.	Mean	S.D.
Right	Cp	-0.2	0.3	0.1	0.3	0.3	0.4	-0.3	0.4	0.1	0.2	0.3	0.3	-0.2	0.3	0.1	0.4	0.2	0.3
	Lp	-0.3	0.5	0.3	0.3	0.2	0.3	-0.2	0.4	0.3	0.5	0.2	0.4	-0.3	0.4	0.3	0.2	0.3	0.3
	Sn	-0.3	0.4	0.2	0.3	0.3	0.2	-0.3	0.5	0.3	0.3	0.3	0.4	-0.4	0.4	0.2	0.4	0.3	0.2
	An	-0.2	0.4	0.4	0.4	0.3	0.4	-0.3	0.6	0.4	0.5	0.3	0.3	-0.2	0.5	0.4	0.4	0.3	0.5
Left	Cp	0.3	0.2	0.3	0.2	0.1	0.3	0.3	0.4	0.3	0.3	0.1	0.4	0.3	0.2	0.3	0.3	0.2	0.3
	Lp	0.2	0.3	0.4	0.5	0.3	0.3	0.2	0.2	0.4	0.3	0.3	0.2	0.3	0.3	0.4	0.3	0.3	0.4
	Sn	0.2	0.4	0.3	0.2	0.4	0.6	0.2	0.3	0.2	0.4	0.3	0.3	0.2	0.4	0.3	0.4	0.4	0.3
	An	0.4	0.5	0.2	0.3	0.3	0.5	0.4	0.3	0.2	0.3	0.3	0.4	0.4	0.4	0.3	0.3	0.3	0.4

(mm)

AO1 : 1 month after SSRO, AO6 : 6 months after SSRO

Lp : Most lateral point of the condylar head of mandible, Sn : Sigmoid notch

Cp : Coronoid process, An : Antegonial notch

Table 5 Changes of condylar head between AO1 and AO6

	Right		Left	
	AO1	AO6	AO1	AO6
SW	7.2 ± 1.2	7.1 ± 1.2	7.9 ± 1.2	7.5 ± 1.2
SH	3.1 ± 0.9	2.4 ± 0.9	3.2 ± 0.7	2.6 ± 0.9
AW	17.4 ± 2.6	17.0 ± 2.8	17.6 ± 2.3	17.1 ± 2.8
AD	7.5 ± 1.2	6.2 ± 1.1	7.9 ± 1.1	7.7 ± 1.1
CW	19.9 ± 2.3	19.8 ± 2.3	20.0 ± 2.3	19.9 ± 2.3
CH	7.8 ± 1.7	6.8 ± 1.7	7.1 ± 1.5	6.2 ± 1.7

**p*<0.05 paired *t*-test (mm)

AO1 : 1 month after SSRO, AO6: 6 months after SSRO

AP : The most anterior point of the condylar head of mandible

PP : The most posterior point of the condylar head of mandible

CoT : The highest point of the condylar head of mandible

SW : The length of AP-PP, SH: The distance from CoT to AP-PP

AW : The length of MP-LP, AD: The distance through the center perpendicular to MP-LP

CW : The length of MP-LP, CH: The distance from CoT to MP-LP

Table 6 Correlations between displacement of proximal bone fragment from BO to AO1 and changes of the condylar head from AO1 to AO6

		SW	SH	AW	AD	CW	CH
Cp	X	0.30	0.06	0.13	0.26	0.42 *	0.53
	Y	-0.39	-0.36	-0.14	-0.48 *	-0.59 *	-0.52 *
	Z	-0.26	-0.17	-0.42 *	0.17	-0.19	0.02
Lp	X	-0.47 *	-0.33	-0.39	-0.47 *	-0.48 *	-0.39
	Y	0.03	0.05	-0.12	-0.02	0.09	0.07
	Z	-0.22	-0.33	-0.32	-0.14	-0.28	-0.16
Sn	X	-0.02	-0.26	-0.04	-0.17	-0.09	-0.10
	Y	-0.21	-0.51 *	-0.21	-0.42 *	-0.33	-0.30
	Z	0.01	-0.23	0.02	-0.03	-0.03	0.02
An	X	-0.29	-0.15	-0.03	-0.37	-0.36	-0.41 *
	Y	-0.34	-0.62 *	-0.37	-0.44 *	-0.43 *	-0.47 *
	Z	0.07	0.08	0.04	0.07	0.14	-0.03

* $p < 0.05$ Pearson's correlation coefficient test

Lp : Most lateral point of the condylar head of mandible, Sn : Sigmoid notch,

Cp : Coronoid process, An : Antegonial notch

AP : The most anterior point of the condylar head of mandible,

PP : The most posterior point of the condylar head of mandible,

CoT : The highest point of the condylar head of mandible

SW : The length of AP-PP, SH : The distance from CoT to AP-PP

AW : The length of MP-LP, AD : The distance through the center perpendicular to MP-LP

CW : The length of MP-LP, CH : The distance from CoT to MP-LP

Table 7 Remodeling of the condylar head from AO1 to AO6

	Remodeling sign(number of condyle = 46)		
	Reductional bony change (%)	Unchanged (%)	Additional bony change (%)
Anteromedial (A)	8 (17.4)	30 (65.2)	8 (17.4)
Anterior-middle (B)	18 (39.1) *	24 (52.2)	4 (8.7)
Anterolateral (C)	19 (41.3) *	21 (45.7)	6 (13.0)
Medial (D)	6 (13.0)	30 (65.2)	10 (21.7) *
Middle (E)	16 (34.8) *	27 (58.7)	3 (6.5)
Lateral (F)	17 (36.9) *	25 (54.3)	4 (8.7)
Posteromedial (G)	8 (17.4)	26 (50.0)	12 (32.6) *
Posterior-middle (H)	4 (8.7)	34 (73.9)	8 (17.4)
Posterolateral (I)	12 (26.0)	25 (54.3)	9 (19.6)

* $p < 0.05$ chi-square test

Unchanged : Less than ± 0.5 mm,

Additional bony change : +0.5mm or more increase

Reductional bony change : -0.5mm or more decrease

Sections were divided into 9 areas : A (Anteromedial), B (Antero-middle), C (Anterolateral), D (Medial), E (Middle), F (Lateral), G (Posteromedial), H (Posteromiddle), I (Posterolateral)
 The changes of the condylar head was evaluated by the least squares method that belong to 3D-superimpose software (Body-Rugle, medic Engineering) using mandibular ramus area.
 The changes of the condylar head were demonstrated by color scale. Chi-square test was performed to compare the ratio of reductional bony change and the ratio of additional bony change in each area.